Pure Appl. Geophys. 179 (2022), 4639–4655

https://doi.org/10.1007/s00024-022-03184-9

Pure and Applied Geophysics

Evaluation of Potential Predictability of Indian Summer Monsoon Rainfall in ECMWF's Fifth-Generation Seasonal Forecast System (SEAS5)

Raju Attada,[1] Muhammad Azhar Ehsan,[2] and Prasanth A. Pillai[3]

Abstract—Forecasts of Indian summer monsoon rainfall (ISMR: June to September, JJAS) are issued prior to the onset of rainy season. Thus, an assessment of both potential and actual forecast skills for Indian summer monsoon rainfall should be based on a longer lead time. Based upon the European Center for Medium Range Weather Forecasts (ECMWF) fifth-generation seasonal forecast system (SEAS5), two lead times are considered: one with an April initial condition (IC) and the other with a May IC from 1981 through 2019 (39 years). Our results show that SEAS5 successfully represents the spatial patterns and variations in the mean JJAS precipitation in the ISMR region compared with the observed rainfall patterns. However, there seem to be significant discrepancies in the simulation of mean precipitation, particularly over topographical regions. SEAS5 is capable of reproducing the observed annual precipitation cycle in India. Moreover, the model is able to better predict the realistic ISMR teleconnections with El Niño-Southern Oscillation and the Indian Ocean Dipole at May ICs. The resulting forecasts across the region are characterized by moderate significant potential and actual skill in both leads, and it decreases as lead time increases. The predictability of SEAS5 is directly related to its ability to correctly predict the forcing of the tropical sea surface temperature and its teleconnections. In spite of this, both lead forecasts have a significant number of unpredicted events and false alarms. This study highlights model discrepancies, shows poor performance in predicting ISMR, and highlights the need for further research on this crucial issue of social relevance.

Keywords: ISMR, ECMWF SES5, predictability, signal, noise, forecast skill.

1. Introduction

As the Indian summer monsoon from June to September (JJAS) contributes more than 80% of the annual total rainfall, seasonal prediction of rainfall at a long lead time is critical (e.g. Rajeevan et al., 2012). Despite recent advances in numerical weather and climate forecasting systems, the prediction of Indian summer monsoon rainfall (ISMR) over large parts of Indian land masses remains a challenging problem, which still appears to be far from a satisfactory solution. Many meteorological centers around the globe are using general circulation models (GCMs) for seasonal prediction (Palmer et al., 2004; Pillai et al., 2018a; Saha et al., 2006, 2014). Many regional studies have evaluated the quality of monthly and seasonal predictions (e.g., Alessandri et al., 2011; Dandi et al., 2020; Kim et al., 2012; Lee et al., 2011; Palmer et al., 2004; Saha et al., 2006; Wang et al., 2009). However, skillful prediction of ISMR has yet to improve for the growing demand for a country like India. The physical deficiencies that cause large uncertainties in the models often limit their seasonal predictive ability. These errors, on the other hand, are model-dependent, and most systematic model biases in seasonal prediction are reported in tropical rainfall, and the effort to explain the physical mechanisms for these biases is ongoing (e.g., Pokhrel et al., 2012; Saha et al., 2013; Chattopadhyay et al. 2015; Pradhan et al. 2017; Pillai et al., 2018a; Singh et al., 2019).

The Indian monsoon region possesses a lower limit on seasonal predictability than the rest of the tropics (Goswami, 1998; Pillai et al., 2018b). Tropical sea surface temperature (SST) variability influenced by the El Niño-Southern Oscillation (ENSO) and the Indian Ocean Dipole (IOD) has a

Supplementary Information The online version contains supplementary material available at https://doi.org/10.1007/s00024-022-03184-9.

[1] Department of Earth and Environmental Sciences, Indian Institute of Science Education and Research (IISER) Mohali, Mohali, Punjab 140306, India. E-mail: rajuattada@iisermohali.ac.in

[2] International Research Institute for Climate and Society, Columbia Climate School, Columbia University, Palisades, New York, NY, USA.

[3] Ministry of Earth Sciences, Indian Institute of Tropical Meteorology, Dr. Homi Bhaba Road, Pashan, Pune 411008, India.

huge impact on ISMR seasonal prediction (e.g., Saji et al., 1999; Ashok et al., 2001; Rao et al., 2010; Dandi et al., 2016; Pillai et al., 2018a, 2018b). Despite significant progress in predicting ISM variability, general circulation models continue to have difficulty simulating seasonal mean ISMR characteristics, intraseasonal variability, and year-to-year variations (e.g., Johnson et al. 2017; Chevuturi et al., 2019). The inability to reproduce interannual variability is mainly due to considerable biases in tropical Indo-Pacific SST and incorrect ENSO-ISMR teleconnections in many global models (Pillai et al., 2018a, 2021). Most seasonal prediction models are also shown to be more dependent on ENSO and IOD-monsoon teleconnections. All of these deficiencies cause the model actual skill to be significantly lower than its potential skill (Krishnakumar et al., 2005; Pillai et al., 2018b). The ISMR skill of the present models is strongly dependent on the model's ability to properly represent ENSO monsoon teleconnection (Jain et al. 2018; Pillai et al., 2018b). To overcome the errors caused by the chaotic nature of the model, the modeling community employs the ensemble forecast approach with lagged initial conditions (e.g., Kumar and Horeling 1995). Further, Wang et al. (2008) reported that the skill of the multi-model ensemble mean is noticeably better than that of individual models.

A new European Centre for Medium-Range Weather Forecasts (ECMWF) seasonal forecasting system 5 (SEAS5) was used to assess the accuracy of predictions of the Indian summer monsoon over two different leads. An earlier intercomparison study by Pillai et al. (2021) using the National Centers for Environmental Prediction (NCEP) Climate Forecast SystemVersion 2 (CFSv2), ECMWF-System4 (previous version of SEAS5) and North American Multi-Model Ensemble (NMME) models had shown that System 4 has a better representation of the mean state of the ISMR, but has insignificant forecasting skill for rainfall during monsoon season. They attributed this difference to the large cold bias (> 2 °C) in the tropical Pacific region, leading to a westward shift in Walker circulation associated with ENSO. Additionally, SEAS5 is more accurate in predicting surface temperatures over the equatorial Pacific and Indian Oceans than System 4 (Johnson et al., 2019). It is essential to examine whether these improvements in SEAS5 reflect better skill for ISM rainfall and associated circulation characteristics. Therefore, this paper aims to explore the skill assessment of ISMR and its predictability in the newly launched SEAS5, with a focus on predicting the monsoon at two different lead times (April and May initial conditions). Recently, Ehsan et al. (2020) also investigated the skill for precipitation in the core summer monsoon region of Pakistan using SEAS5 and NMME models based on initial conditions in June, May, and April. They found that SEAS5 outperformed the NMME models; however, the skill obtained was quite low. Paparrizos et al. (2021) verified the SEAS5 seasonal prediction data against ground observations over the lower Ganges Delta during the monsoon period and found lower skill during the monsoon period.

2. *Data and Methodology*

This study makes use of the ECMWF seasonal forecast system 5 (ECMWF's 43r1 Integrated Forecasting System Cycle) database. SEAS5 has an upgraded ocean component, high spatial resolution (36 km and 91 vertical levels), and an updated land surface scheme (Johnson et al., 2019). NEMO ((Nucleus for European Modelling of the Ocean, v3.4.1) is used as an ocean model at 0.25° horizontal resolution and has 75 layers, with 18 layers in the first 50 m. Readers are encouraged to review Johnson et al. (2019) and their references for additional information regarding the various upgrades. A forecast of "Lead-1" is based on initial conditions of May, while the forecast of "Lead-2" is based on initial conditions of April. In this study, 25 ensemble members are used for the period 1981–1999 (39 years), common for both the hindcast (1981–2016) and forecast (2017–2019) periods.

The Climate Prediction Center Merged Analysis of Precipitation (CMAP) is obtained from five different satellite estimates and the station data set available at spatial resolution of 2.5° × 2.5° (Xie & Arkin, 1997), and station-based gridded rainfall from the India Meteorological Department (IMD; 0.25° × 0.25°) is also used (Pai et al., 2014). The SST data are obtained from the Hadley Centre Sea

Ice and Sea Surface Temperature data set (HadISST) at 1° × 1° horizontal resolution (Rayner et al., 2003). Circulation data are obtained from ERA5, available at 0.25° resolution (Hersbach et al., 2018). We converted observation and prediction data sets to a common resolution (1° × 1°) using bilinear interpolation.

The CMAP observed rainfall was used in conjunction with various statistical skill scores in order to evaluate the SEAS5 predicted rainfall. Furthermore, the computation of model's predictive skill closely follows the work by Ehsan et al. (2017b, 2019). Potential predictability is calculated as the ratio of signal and noise variances where the "signal" represents the mean component of the ensemble and "noise" is related to the internal dynamics of the system. The potentially predictable quantity signal and the unpredictable noise portion are calculated as described in Eqs. 1 and 2 in Kang et al. (2004a, 2004b). The perfect model correlation (PMC) is used to assess the predictability of summer mean precipitation (e.g., Ehsan et al., 2013; Kang et al., 2006). Finally, the Student *t*-test is used to determine the significance of the results (Wilks, 2006).

3. Results and Discussion

3.1. SEAS5 Simulation of ISMR Mean and Variability

As a first step, we analyze the mean rainfall during the Indian summer monsoon in SEAS5. It is noticeable that the Western Ghats (orography-induced) and the monsoon core region obtain a maximum portion (90%) of the total annual rainfall, whereas the rain shadow region (southern) and northwestern India receive relatively less (50–75%) rainfall during the monsoon season (Fig. 1). The SEAS5 simulated rainfall (Fig. 1b) contribution/fraction agrees well with the observations.

Furthermore, we examine the simulation of the mean rainfall of JJAS from the hindcasts with a 1-month (May IC) and 2-month lead time (i.e., April IC) against observations. The seasonal mean precipitation observed (Fig. 2a) (June–July–August–September, JJAS) exhibits maximum rainfall in three locations, namely, northeast India, the Western Ghats, and the monsoon core region. The ensemble mean of the SEA5 models reasonably simulates the locations of the maximum rainfall over India in both the April IC (Fig. 2b) and the May IC (Fig. 2b) with smaller differences. For both initial conditions, the SEAS5-derived climatology captures well the minimum rainfall band over northwest India and the southern peninsula (e.g., Tamil Nadu and adjoining regions). In comparison with observations, SEAS5 shows slightly higher rainfall in northeastern India and the Himalayas. It should be emphasized that the interplay of the ISM and the Himalayas is vital to many climatological aspects of the Himalayan foothill and foreland regions, which is quite complex in capturing this in the current climate models. SEAS5 overestimated the rainfall over the Himalayas and Western Ghat regions compared with CMAP, as with other contemporary seasonal forecast models such as the NMME seasonal systems (e.g. Chevuturi et al., 2021; Singh et al., 2019). These orographic regions have known difficulties in representing orographic precipitation (e.g. Pokhrel et al., 2016) and irrigation in surface processes, which often play a key role in such rainfall errors. Importantly, however, we should be cautious of the fact that the observations over the high orography have large uncertainties due to sparse observational networks.

Figure 2 (right panel) depicts the spatial distribution of the standard deviation of the observations, the ICs of April (L-2) and May (L-1) during JJAS. Based on the spatial distribution of the ensemble mean standard deviation of the mean summer precipitation, the observed rainfall variability is particularly high on the west coast of India, the monsoon core region, and the northeastern region of India (Fig. 2c). SEAS5 captures the interannual variability in JJAS rainfall on both lead times (Fig. 2e, f), in a similar manner to the observations. However, SEAS5 overestimates the observed rainfall. We further evaluated SEAS5 predicted mean rainfall with the IMD rainfall as shown in Figure S1. It is found that SEAS5 qualitatively matches with the high resolution IMD data albeit some magnitude differences. Comparison of these two figures indicates that both rainfall data capture the major features of monsoon rainfall over

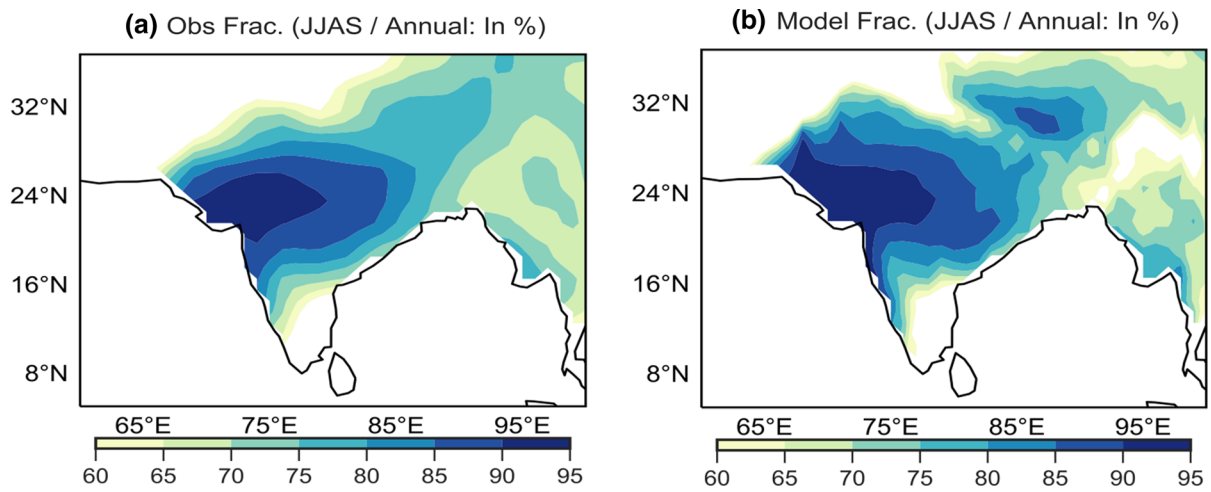

Figure 1
Percentage contribution of summer monsoon (JJAS) rainfall to annual rainfall from (**a**) observations (CMAP) and (**b**) SES5 ensemble mean for the period 1981–2019

Indian land region. Additionally, the difference in rainfall between the ensemble mean and the observations at L-1 and L-2 (Fig. 3) suggests that the model is biased wet over the Western Ghats and central and northeast Indian regions. The bias patterns of the two leads are very similar. In the case of RMSE, SEAS5 exhibits high rainfall errors over the mountain regions for both leads. Similar results are obtained when IMD rainfall data are used for the evaluation (Fig. S3). We further construct the annual cycle for L-1 and L-2 hindcasts by considering initializations every month to assess the model fidelity in monsoon rainfall evolution. The annual precipitation cycle of SEAS5 over the Indian subcontinent is distinguished by a dramatic rise in rainfall in May and a subsequent decline from September onwards. The observed mean annual cycle is depicted well by SEAS5 hindcasts (Fig. 4), albeit with some differences (overestimated). Some studies have reported that models with better seasonal mean rainfall patterns have better skill in seasonal prediction (e.g., Delsole & Shukla, 2010). In addition, studies have shown that better tropical Pacific teleconnections within coupled models can also contribute to better seasonal prediction accuracy (e.g., Ehsan et al., 2017a; Pillai et al., 2021).

3.2. Assessment of Interannual Variability

The interannual variations in ISMR are critical because they have a huge impact on many sectors including agriculture production. We will be specifically analyzing the interannual variability in ISMR, based on the ICs of April and May of SEAS5. In Fig. 5, we show the time series of ISMR anomalies for observations and model hindcasts at two different leads for the entire country of India (Fig. 5a) and the central part of India (Fig. 5b). During the SEAS5 hindcast period, there are eight excess monsoon years (more than one SD; 1988, 1990, 2005, 2007, 2008, 2010, 2011, 2013) and six deficient monsoon years (less than one SD; 1982, 1984, 1989, 2002, 2009, 2014) observed (Table 1). For ISMR, it can be observed that May IC has an exceptionally high prediction skill (0.47), catching most of the excess and deficient monsoon years, whereas April IC shows a noticeably lower prediction skill (0.36). Interestingly, in central India, the prediction skill of SEAS5 is lower than the average rainfall of all of India for the April ICs (0.34) and the May ICs (0.29), following earlier studies. The lower skill for ISMR in SEAS5 is related to large cold bias in the equatorial central and eastern Pacific Ocean, and the hindcasts with large cold bias in these basins have a La Niña type structure of bias and has close to the

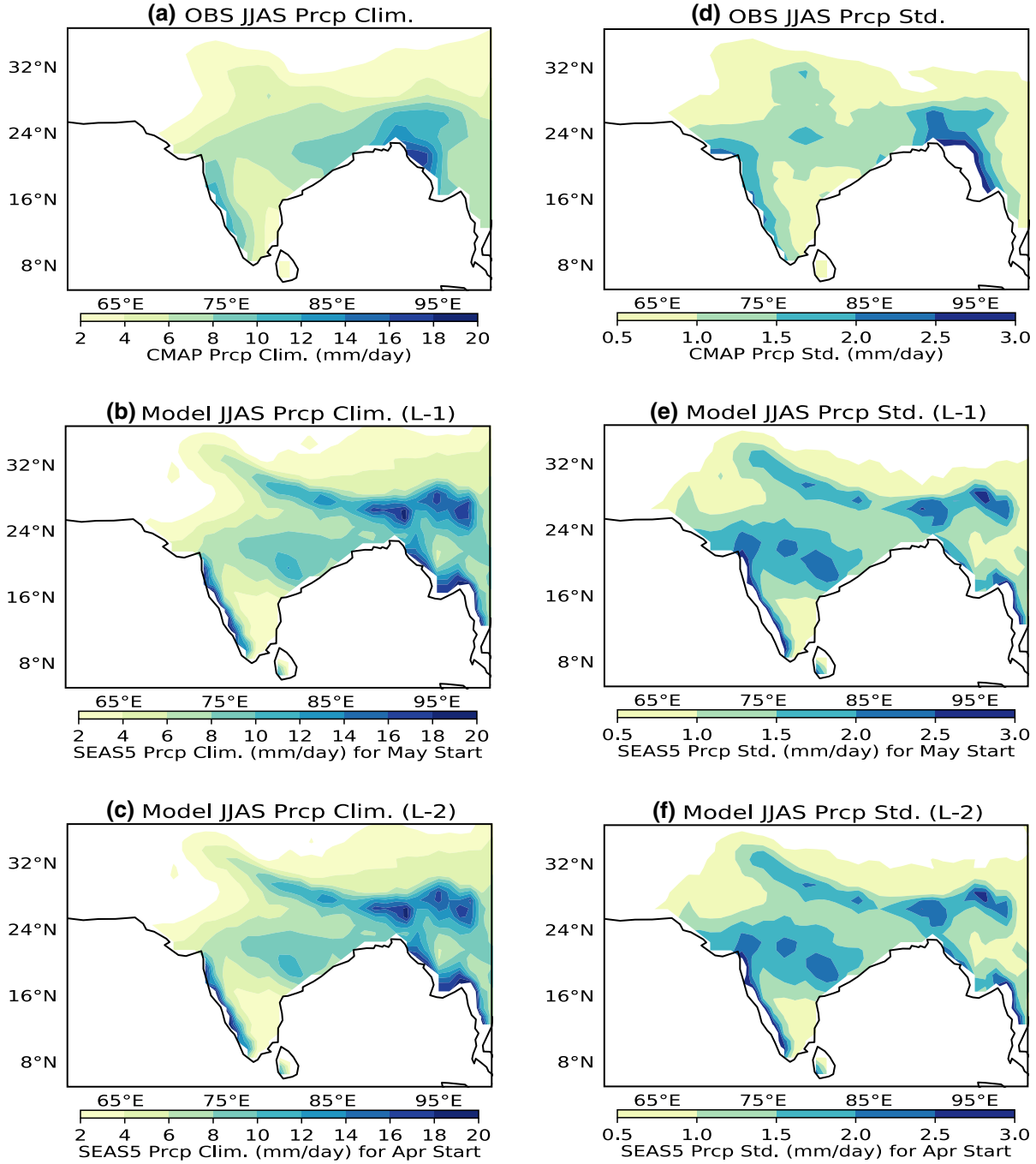

Figure 2

The observed (CMAP) and predicted precipitation climatology (**a**, **b**, **c**) during monsoon season (JJAS) for the period 1981 to 2019. The standard deviation of JJAS precipitation from observations (**d**) and SEAS5 with (**e**) May (Lead-1) and (**f**) April (Lead-2) start dates. The standard deviation in (**e**, **f**) is calculated from all ensemble members and all years. Unit of precipitation is mm/day

observed mean ISMR distribution and annual cycle. It is important to note that Fig. 5 shows a significant number of El Niño years such as 1984, 1989, 2002 and 2009 but no reduced rainfall for the models

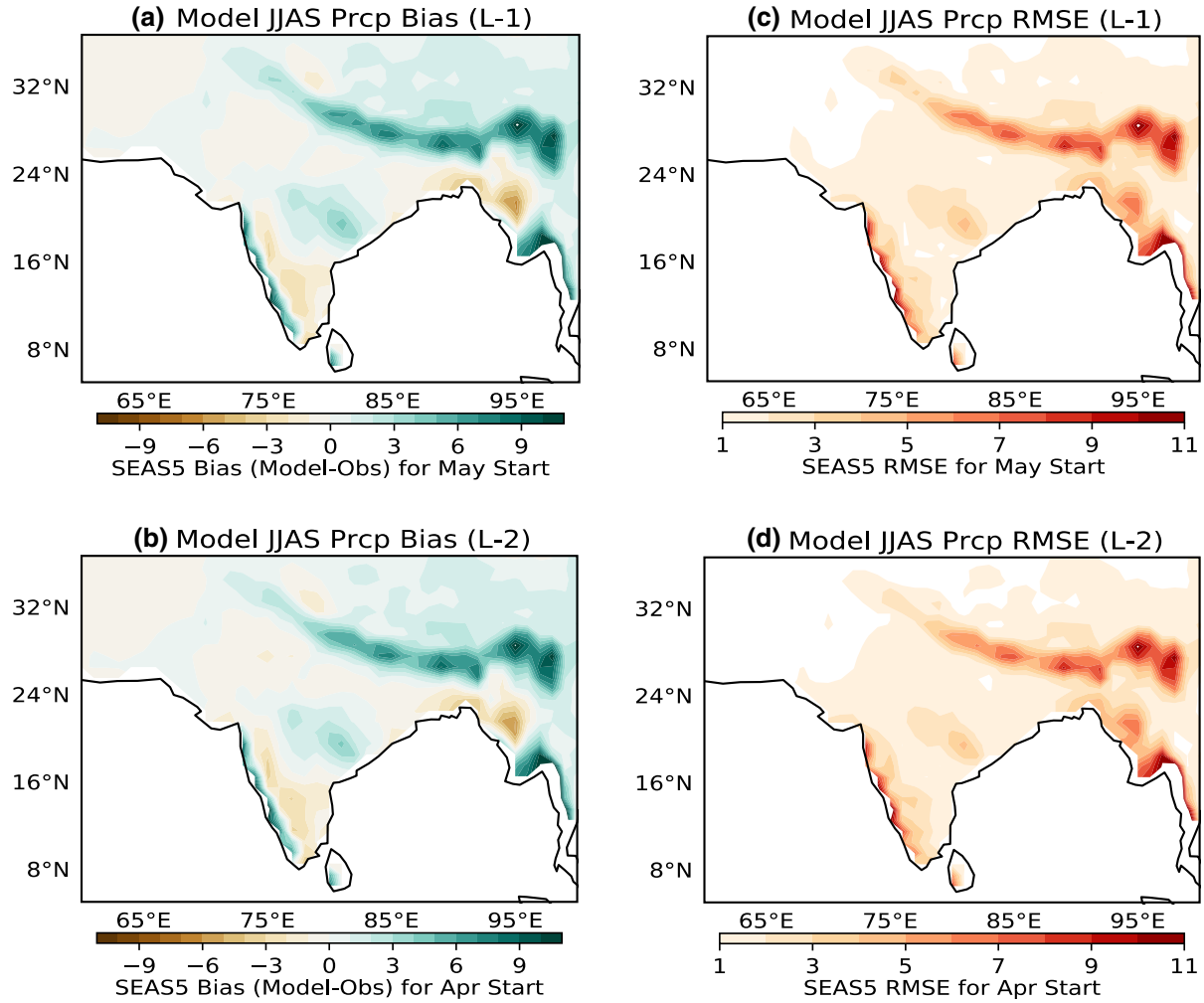

Figure 3
JJAS mean rainfall biases (mm/day) and root mean square error (mm/day; RMSE) between SEAS5 (L-1; L-2) and observations

resulting in false alarms and lower hindcast skill. We are now looking into large-scale control of ISMR because interannual variations in ISMR are substantially influenced by large-scale climate drivers such as ENSO (Pillai et al., 2018a).

Figures 6 and 7 show the spatial distribution of the composites of excess and deficient rainfall anomalies as computed from observations and from the ensemble means of the model over the Indian region. Observations show a strong positive (negative) rainfall anomaly in India during the years of excess (deficit) monsoons. During the excess (deficit) monsoon years, the spatial distribution of SST anomalies (Fig. 6c, d) displays colder (warmer) than normal anomalies across the central and eastern equatorial Pacific, with an elongated cold (warm) tongue extending west of the dateline. During excess (deficit) years, the central and western Pacific experience strong easterly (westerly) wind anomalies. According to Singh et al. (2014), weak circulation patterns in the Arabian Sea is predominant during deficit monsoon years as a result of large-scale circulations from the Pacific. This clearly indicates a destabilization of the Somali jet and is similar to the Pacific's rebuttal to large-scale El Niño forcing (e.g., Chowdary et al., 2006; Joseph & Sijikumar, 2004). The atmospheric circulation response to eastern Pacific cooling (warming) is well structured along

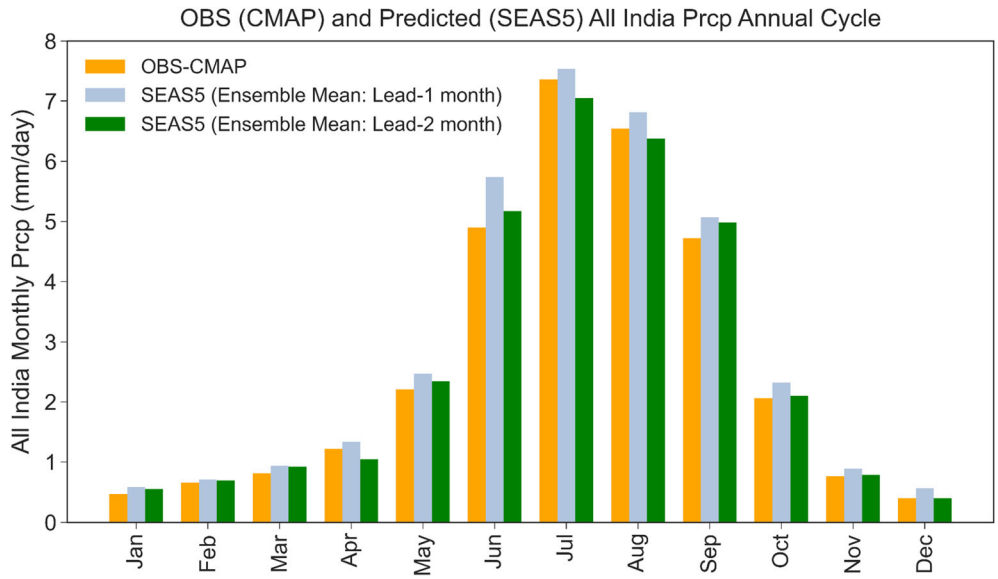

Figure 4
Annual cycle of rainfall (mm/day) from observations (CMAP) and model (SEAS5) at two different leads (L-1 and L-2). For instance, Lead-1 for Sep, Oct, and Nov months show forecast initialized in Aug, Sep, and Oct, while Lead-2 show forecasts initialized in Jul, Aug, and Sep, respectively

the equator. In excess (deficit) years, geopotential height anomalies at low levels (850 hPa) over the tropical Indian Ocean (TIO) and the Western Ghats tend to be negative (positive), indicating large-scale convective activity (subsidence) in this area (Fig. 6e, f). These observed composite features are well predicted with the May IC, as compared with the April IC predictions. In May IC, SEAS5 (Fig. 7) could predict a dominant rainfall anomaly over the whole country. It appears that equatorial SST anomalies are confined to the eastern equatorial Pacific with an elongated cold (warm) tongue extending westward from the south American coast, and low-level (850 hPa) wind anomalies in the eastern Pacific are divergent (convergent), respectively, during excess (deficit) monsoon years. Similar spatial distributions are obtained with April ICs (Fig. S4) but with significantly lower skill.

3.3. *Potential Predictability and Skill for ISMR in SEAS5*

As part of this section, we analyze the model's ability to predict the actual and potential skill of rainfall during the Indian summer monsoon. The actual skill is defined as the mean of the ensemble members and the observations, whereas the potential skill represents the maximum skill of the model and is independent of the observations. Figure 8 shows the potential and actual skill of the hindcasts for May IC (Fig. 8a, c) and April IC (Fig. 8b, d). The potential skill is highest in the central monsoon region (> 0.6) for May IC, followed by the southern peninsular region (Fig. 8a) and decreased with an increase in lead time to L-2, mainly in the southern peninsular and northwest region (Fig. 8b), but the maximum correlation persists in the central monsoon region. The actual skill is lower than the potential skill, but the maximum skill is in the central core monsoon region with a value of around 0.4 for both hindcasts (Fig. 8c, d). Actual skill is also higher for short-lead than long-lead hindcasts, considering India as a whole, but more grids have a higher correlation of 0.4 in the central monsoon region for April IC. Meanwhile, the correlation is negligible in the southern peninsula region for May IC, which has a higher value for potential skill. Based on this difference between potential and actual skill, it is evident that there is room for improvement in the model. This can be achieved by many improvements,

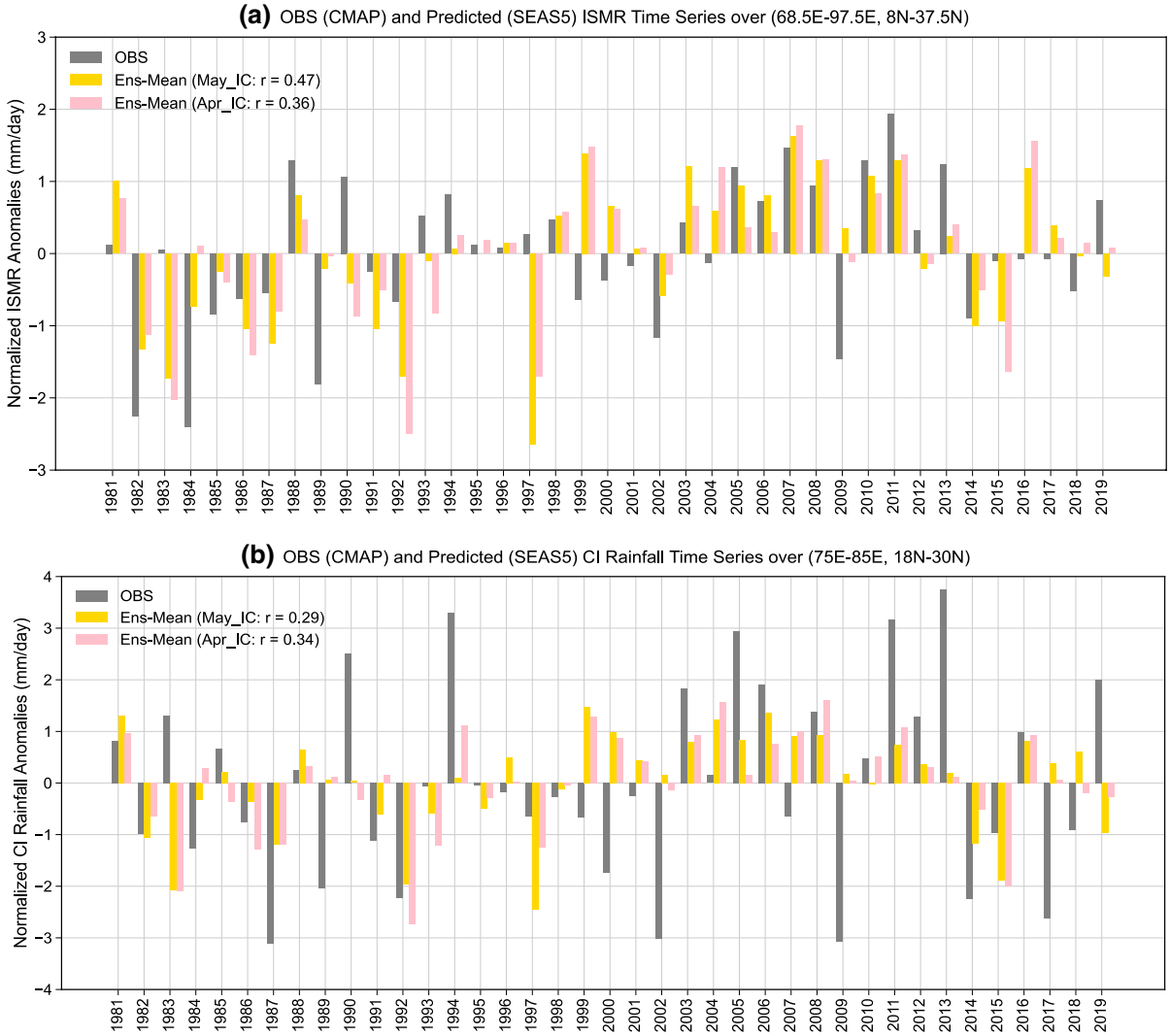

Figure 5

Interannual variations in summer monsoon rainfall anomalies for (**a**) all India, and (**b**) central Indian regions in SEAS5 and observations. Correlation between the CMAP and model-predicted rainfall averaged over the Indian subcontinent is outlined in the top left corner. The value higher than 0.32 shows statistically significant correlation coefficient at 95% confidence level

Table1

Excess and deficit years

Category	Years
Excess	1988, 1990, 2005, 2007, 2008*, 2010, 2011, 2013
Deficit	1982, 1984, 1989, 2002, 2009, 2014*

*Considered very close to the threshold value

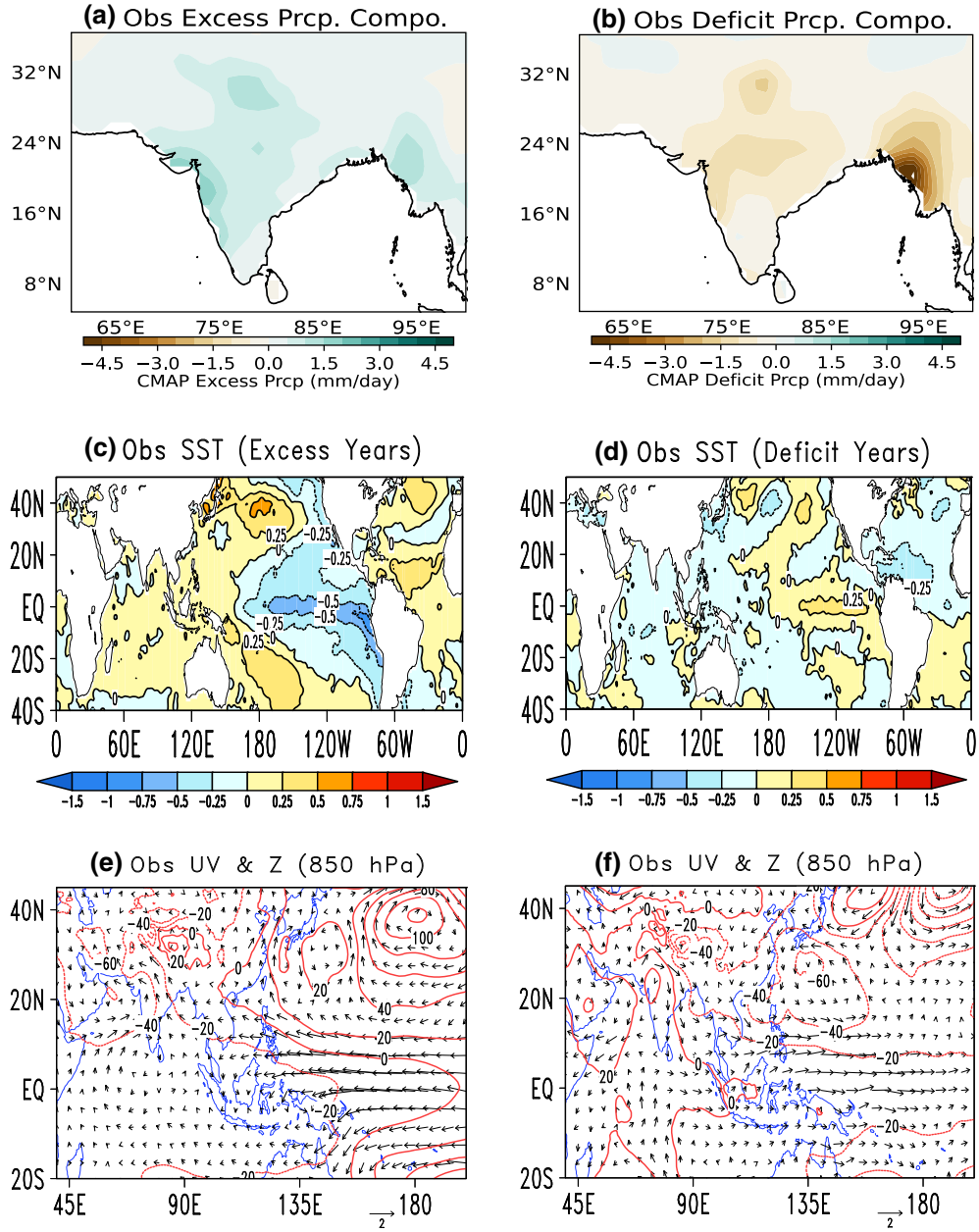

Figure 6
Observed precipitation (**a, b**), sea surface temperature (**c**, **d**) and (**e**, **f**) lower level (850 hPa) winds (vectors) and geopotential height (m) during excess and deficit monsoon years

such as physical parameterizations (e.g., Ehsan et al., 2017b; Ehsan et al. 2017c), dynamical data assimilation techniques, and statistical post-processing techniques (e.g., Acharya et al., 2021), and this is not part of the present study.

The potential skill of rainfall can also be interpreted from its ability to properly represent the signal by reducing the noise. Signal represents the mean component of the ensemble of the rainfall, while noise represents the spread between ensembles

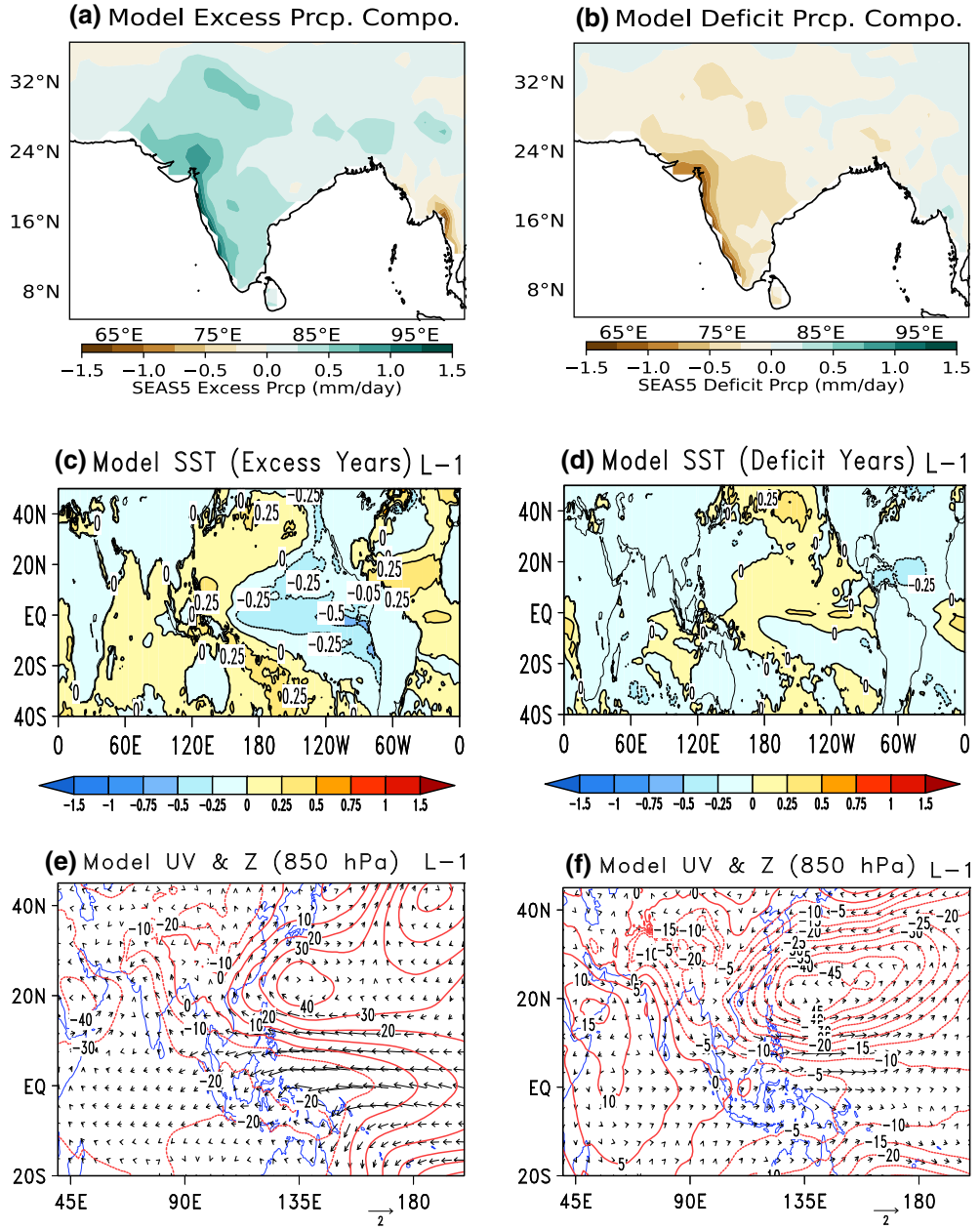

Figure 7
Same as Fig. 6 but for the model at May IC (L-1)

of the model. Figure 9 shows the signal (Fig. 9a, b), noise (Fig. 9c, d), along with signal-to-noise ratio (Fig. 9e, f) for May IC and April IC model hindcasts. Across the Indian land region, both hindcasts show a very weak signal compared with the noise, indicating that it is difficult to capture the variability in the Indian land region in hindcasts. The signal is prominent in the southwestern region, followed by the north-central and eastern regions for both hindcasts. Noise is also noticeable in these regions, but it is also maximum over the land region between 16° and 24°N. On the basis of two hindcasts (April and

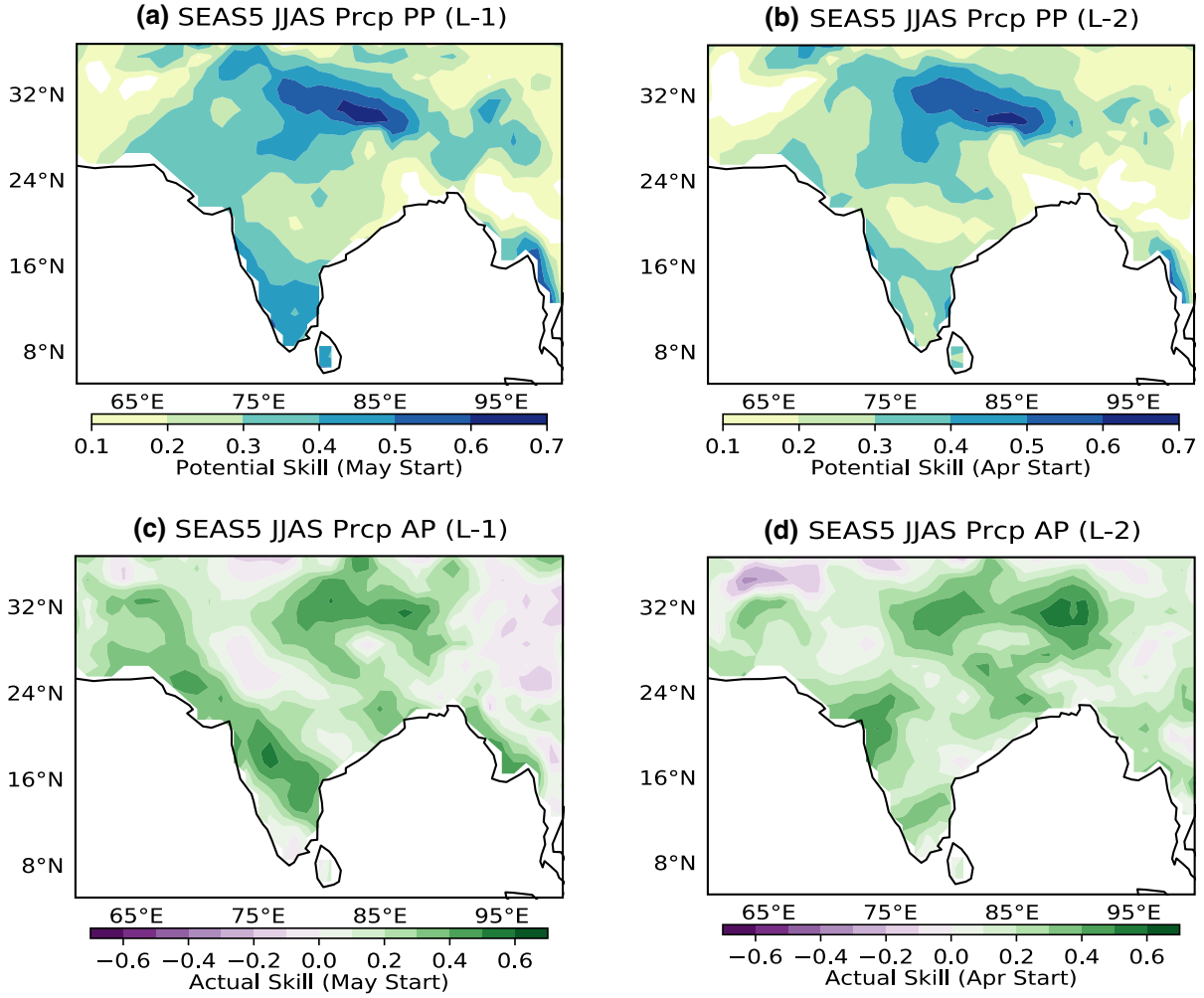

Figure 8
Spatial distribution of potential skill (**a**, **b**) and actual skill (c and d) between observation and SEAS5 ensemble mean precipitation initialized at (**a**) May (L-1), and (**b**) April (L-2), respectively. In (**c**, **d**), the value higher than 0.32 shows a statistically significant correlation coefficient at 95% confidence level

May ICs) of monsoonal rainfall over Indian land, the SEAS5 model exhibits good potential skill in the central parts of the country. Our analysis indicates that model skill is higher in areas with a higher signal-to-noise ratio, or in regions where the signal predominates over the noise.

4. Evaluation of Tropical SST Teleconnections

ISMR variability is mainly associated with ENSO in the Pacific (e.g., Kumar et al., 1999; Rajeevan & Pai, 2007; Dandi et al., 2016; Pillai et al., 2018a, 2018b) and the Dipole Mode in the Indian Ocean (IOD: Saji et al., 1999; Ashok et al., 2004). Therefore, the importance of addressing those teleconnections in SEAS5 cannot be overstated because having the right teleconnections is an important part of producing reliable seasonal forecasts (e.g., Ehsan, 2020; Ehsan et al., 2021). Figure 10 displays the correlation between JJAS Niño 3.4 SST and global tropical SSTs. The pattern correlation coefficient (PCC) between observed and model teleconnections is represented by the value on the right side of each

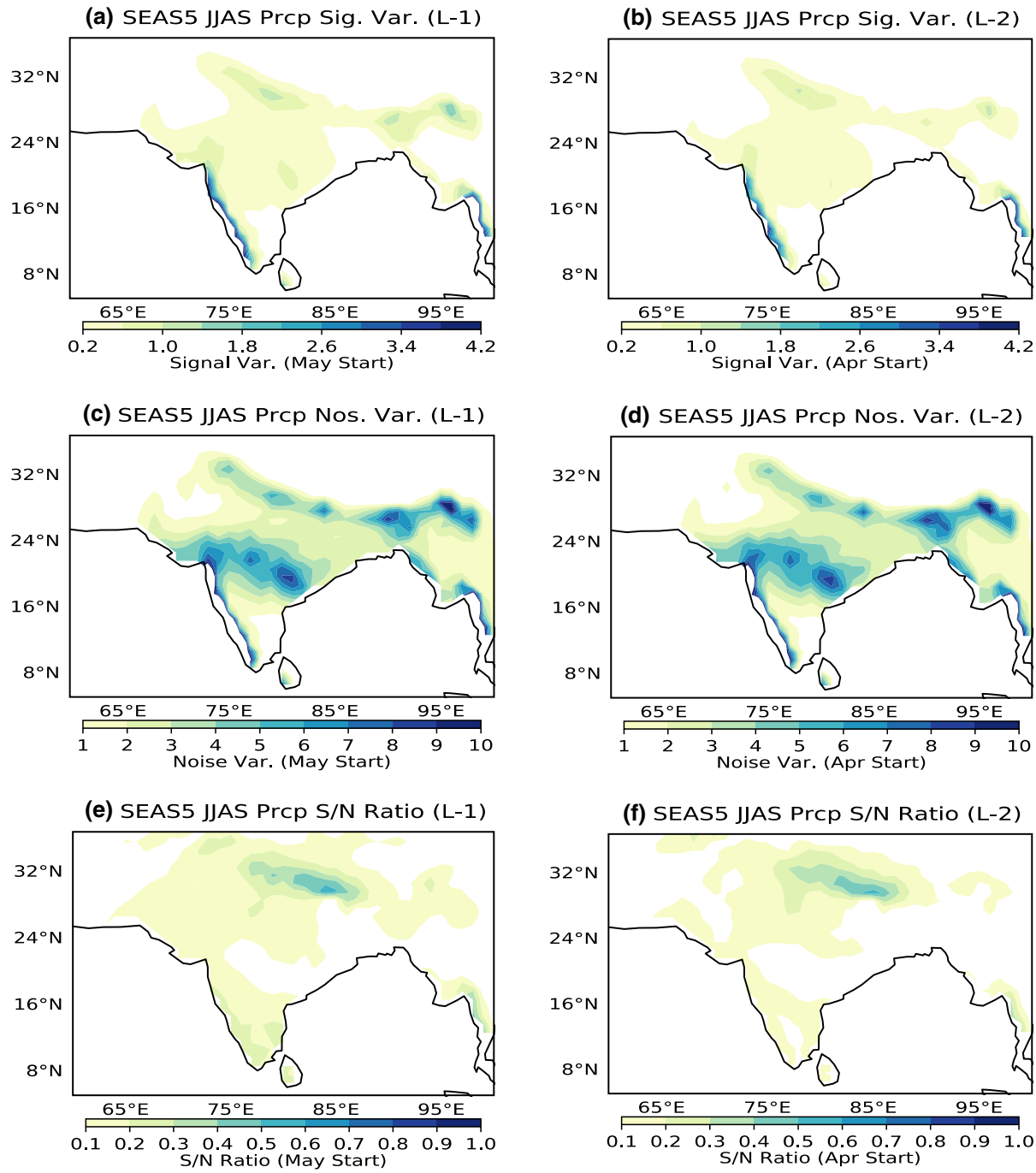

Figure 9
Spatial distribution of signal, noise, and signal-to-noise ratio between observations and ensemble mean precipitation from SEAS5 initialized at (**a**) May, and (**b**) April, respectively

panel. Observations (Fig. 10a) exhibit positive association in the eastern and central tropical Pacific and negative correlations in the western tropical Pacific. SEAS5 predicts this large-scale teleconnection

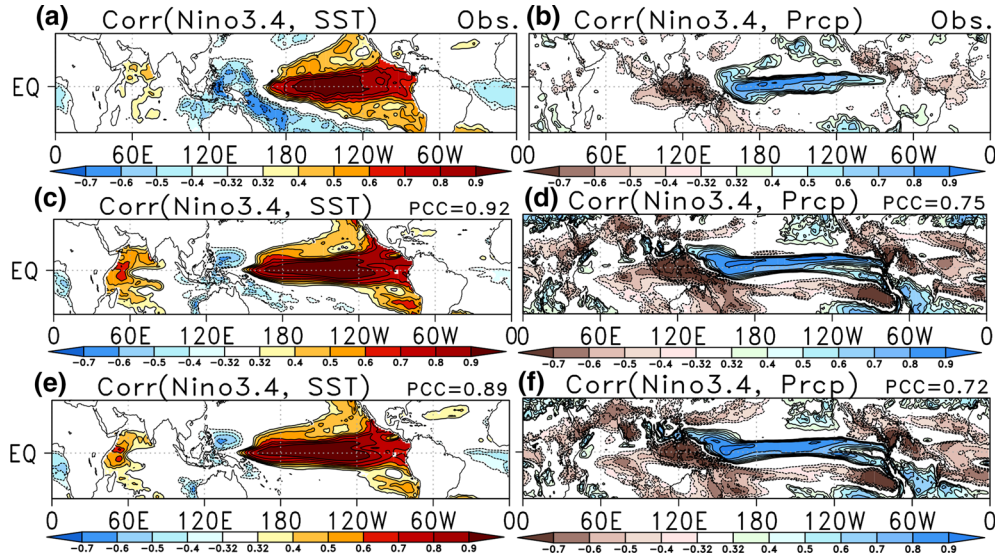

Figure 10
Correlation between observed JJAS Niño3.4 index and SST anomalies for observations (**a**), May ICs (**c**; L-1), and April ICs (**e**; L-2). Correlation between observed Niño3.4 index and precipitation anomalies for observations (**b**), May ICs (**d**; L-1), and April ICs (**f**; L-2). A value higher than 0.32 shows a statistically significant correlation coefficient at 95% confidence level

pattern associated with Niño 3.4 SSTs over the tropical oceans for both May (Fig. 10c) and April ICs (Fig. 10e). The correlation patterns are observed to be greater in the case of May IC (0.92) than in April IC (0.89), indicating a better skill obtained with May ICs. Figure 10 depicts a spatial correlation map between Niño 3.4 SSTs and rainfall during boreal summer-time. The Niño 3.4 SST anomalies were found to be significantly associated (negatively) with monsoon rainfall in India (Fig. 10b). Furthermore, negative correlations are also detected across the Indian landmass in both April and May ICs (Fig. 10d, f). SEAS5 successfully predicted this negative relation between Niño 3.4 and Indian rainfall during the monsoon season with both April and May ICs. However, it is slightly overestimated in SEAS5 compared with observations. It is quite common for various prediction systems to predict a stronger ENSO-monsoon relationship (e.g., Dandi et al. 2016; George et al. 2016). It should also be noted that the strong positive correlation between Niño 3.4 anomalies and rainfall over the tropical Pacific is reflected in SEAS5 for both leads though with a degree of overestimation.

As part of the assessment, we examine how well SEAS5 predicts the relationship between the IOD and tropical SSTs and rainfall. As shown in Fig. 11, the DMI index is spatially correlated with tropical SSTs. There is a positive correlation between the eastern and central Pacific regions, whereas the equatorial warm pool area and the eastern TIO exhibit a negative relationship (Fig. 11a). These teleconnection patterns were predicted more successfully in May ICs (Fig. 11c) than in April ICs, where the relationship started to fade slightly. There is a pattern correlation coefficient of approximately 0.57 for the May ICs (Fig. 11d), which indicates that there is a good correlation between IOD and tropical rainfall in the model. SEAS5 is able to predict these relationships, but the correlations are slightly weaker with April ICs than with May ICs. Importantly, one of the major improvements in SEA5 for IOD teleconnection is that the model successfully captures the dipole SST pattern. Furthermore, the model induced precipitation over the monsoon region which is comparable to observed patterns. Hence, the model is able to properly simulate the teleconnection from the tropical Pacific as well as the Indian Ocean. There is a better PCC for teleconnections in May than its counterpart

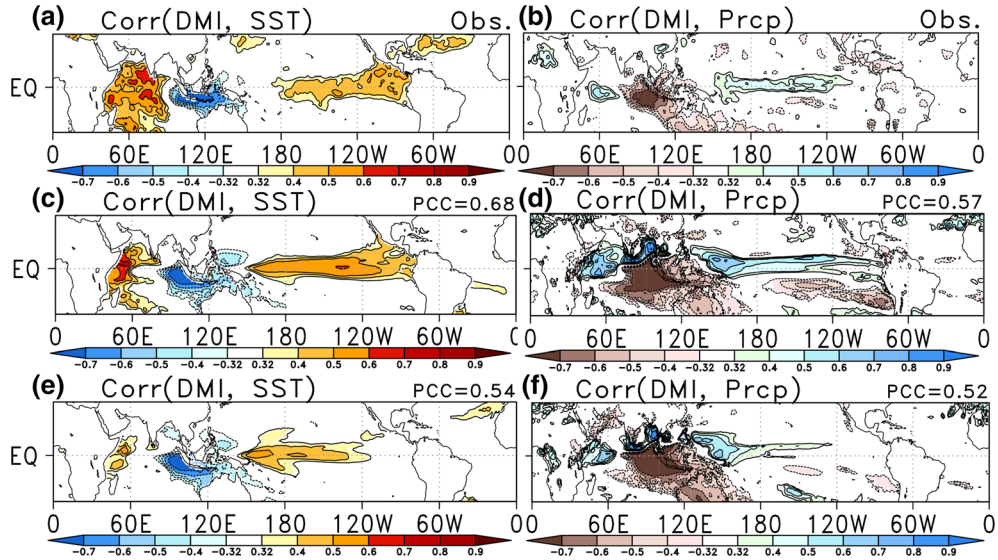

Figure 11
Same as Fig. 10 but with Indian Ocean Dipole

in April, resulting in better predictability of the ISMR.

5. Summary and Conclusions

The skill of long-range seasonal ISMR prediction has significant social and economic implications, including the ability to replenish reservoirs and groundwater, allowing better irrigation and increased agricultural production. As a matter of fact, it is critical to undergo regular checks on the next-generation coupled seasonal prediction models. This study evaluates the performance among the most recent coupled ensemble seasonal forecast system (ECMWF SEAS5) in predicting monsoon rainfall over India. The following are the important takeaways from this analysis.

1. Seasonal mean monsoon precipitation patterns over the Western Ghats, monsoon core region, northeast India, and the Himalayas are successfully simulated by the SEAS5 model (ensemble mean). Furthermore, SEAS5 exhibits relatively better skill in predicting large-scale monsoon circulation patterns during ISM with May and April ICs, but with May ICs it performs better.
2. The spatiotemporal variability in the Indian summer monsoon rainfall is well represented in SEAS5 in both leads (May and April ICs).
3. SEAS5 can capture the interannual variability in ISMR reasonably well with both leads.
4. The SEAS5 models have moderate potential skill in predicting the summer monsoon rainfall over the Indian land region in both hindcasts, and the maximum skill is obtained in the central Indian region.
5. SEAS5 is able to properly predict the large-scale teleconnection of tropical SST with ISMR.
6. Better teleconnection of tropical SSTs with ISMR makes May IC hindcasts more skillful than April IC.
7. Actual skill is also higher for short-lead than long-lead hindcasts, considering India as a whole, but more grids have a higher correlation of 0.4 in the central monsoon region for April IC.

Acknowledgements

We acknowledge the Copernicus Climate Data Store for providing System-5 data. The reanalysis hindcasts of SEAS5 and ERA5 (https://doi.org/10.24381/cds.

6860a573) are publicly available from the Copernicus Climate Change Service (C3S) of the ECMWF, through its climate data store. SEAS5 data can be downloaded from the Copernicus Climate Data Store (https://cds.climate.copernicus.eu/cdsapp#!/dataset/seasonal-monthly-single-levels?tab=form).

Author Contributions RA and MAE designed the project and wrote most of the paper. They worked on part of the computations and drew most of the figures; Prasanth helped in writing and editing the article.

Funding

The study was not funded by an external grant.

Data availability

The data sets generated during and/or analyzed during the current study are available publicly and are also provided in the manuscript as well as in the acknowledgements section.

Declarations

Conflict of interest The authors have no conflicts of interest to declare.

Code availability Not applicable.

Ethical approval and consent to participate The authors confirm that this study is a new investigation that has not been published previously.

Consent for publication Not applicable.

References

Acharya, N., Ehsan, M. A., Admasu, A., Teshome, A., & Hall, K. J. C. (2021). On the next generation (NextGen) seasonal prediction system to enhance climate services over Ethiopia. *Climate Services, 24*, 100272. https://doi.org/10.1016/j.cliser.2021.100272

Alessandri, A., Borrelli, A., Navarra, A., Arribas, A., Déqué, M., Rogel, P., & Weisheimer, A. (2011). Evaluation of probabilistic quality and value of the ENSEMBLES multimodel seasonal forecasts: Comparison with DEMETER. *Monthly Weather Review, 139*(2), 581–607. https://doi.org/10.1175/2010MWR3417.1

Ashok, K., Guan, Z., & Yamagata, T. (2001). Impact of the Indian Ocean Dipole on the relationship between Indian monsoon rainfall and ENSO. *Geophysical Research Letters, 28*(23), 4499–4502. https://doi.org/10.1029/2001GL013294

Chattopadhyay, R., Rao, S. A., Sabeerali, C. T., George, G., Rao, D. N., Dhakate, A., & Salunke, K. (2016). Large-scale teleconnection patterns of Indian summer monsoon as revealed by CFSv2 retrospective seasonal forecast runs. *International Journal of Climatology, 36*(9), 3297–3313. https://doi.org/10.1002/joc.4556

Chevuturi, A., Turner, A. G., Johnson, S., Weisheimer, A., Shonk, J. K., Stockdale, T. N., & Senan, R. (2021). Forecast skill of the Indian monsoon and its onset in the ECMWF seasonal forecasting system 5 (SEAS5). *Climate Dynamics, 56*(9), 2941–2957. https://doi.org/10.1007/s00382-020-05624-5

Chowdary, J. S., Gnanaseelan, C., Sinha, S. K., & Thompson, B. (2006). A study on the variability of atmospheric and oceanic processes over the Arabian Sea during contrasting monsoons. *Meteorlogical Atmosphere Physics, 94*(1), 65–85. https://doi.org/10.1007/s00703-005-0166-3

Dandi, A. R., Pillai, P. A., Chowdary, J. S., Desamsetti, S., Srinivas, G., Rao, K. K., & Nageswararao, M. M. (2020). Inter-annual variability and skill of tropical rainfall and SST in APCC seasonal forecast models. *Climate Dynamics, 56*(1), 439–456. https://doi.org/10.1007/s00382-020-05487-w

Delsole, T., & Shukla, J. (2010). Model fidelity versus skill in seasonal forecasting. *Journal of Climate, 23*(18), 4794–4806. https://doi.org/10.1175/2010JCLI3164.1

Ehsan, M. A. (2020). Potential predictability and skill assessment of boreal summer surface air temperature of South Asia in the North American multimodel ensemble. *Atmospheric Research, 241*, 104974. https://doi.org/10.1016/j.atmosres.2020.104974

Ehsan, M. A., Almazroui, M., & Yousef, A. (2017c). Impact of different cumulus parameterization schemes in SAUDI-KAU AGCM. *Earth Systematic Environment, 1*, 3. https://doi.org/10.1007/s41748-017-0003-0

Ehsan, M. A., Almazroui, M., Yousef, A., Enda, O. B., Tippett, M. K., Kucharski, F., & Alkhalaf, A. A. (2017b). Sensitivity of AGCM-simulated regional summer precipitation to different convective parameterization schemes. *International Journal of Climatology, 37*(13), 4594–4609. https://doi.org/10.1002/joc.5108

Ehsan, M. A., Kang, I. S., Almazroui, M., et al. (2013). A quantitative assessment of changes in seasonal potential predictability for the twentieth century. *Climate Dynamics, 41*, 2697–2709.

Ehsan, M. A., Kucharski, F., & Almazroui, M. (2019). Potential predictability of boreal winter precipitation over central-

southwest Asia in the North American multi-model ensemble. *Climate Dynamics, 54*, 473–490. https://doi.org/10.1007/s00382-019-05009-3

Ehsan, M. A., Tippett, M. K., Almazroui, M., Ismail, M., Yousef, A., Kucharski, F., Omar, M., Hussein, M., & Alkhalaf, A. A. (2017a). Skill and predictability in multimodel ensemble forecasts for Northern Hemisphere regions with dominant winter precipitation. *Climate Dynamics, 48*(9–10), 3309–3324.

Ehsan, M. A., Tippett, M. K., Kucharski, F., Almazroui, M., & Ismail, M. (2020). Predicting peak summer monsoon precipitation over Pakistan in ECMWF SEAS5 and North American Multimodel Ensemble. *International Journal of Climatology, 40*(13), 5556–5573. https://doi.org/10.1002/joc.6535

Ehsan, M. A., Tippett, M. K., Robertson, A. W., Almazroui, M., Ismail, M., Dinku, T., Acharya, N., Siebert, A., Ahmed, J. S., & Teshome, A. (2021). Seasonal predictability of Ethiopian Kiremt rainfall and forecast skill of ECMWF's SEAS5 model. *Climate Dynamics, 57*(11–12), 3075–3091. https://doi.org/10.1007/s00382-021-05855-0

Goswami, B. N. (1998). Interannual variations of Indian summer monsoon in a GCM: External conditions versus internal feedbacks. *Journal of Climate, 11*(4), 501–522. https://doi.org/10.1175/1520-0442(1998)011%3c0501:IVOISM%3e2.0.CO;2

Hersbach H, Dee D (2016) ERA5 reanalysis is in production. ECMWF Newsletter. 147:7. https://www.ecmwf.int/en/newsletter/147/news/era5-reanalysis-production/ (accessed 14 November 2018).

Johnson, S. J., et al. (2019). SEAS5: The new ECMWF seasonal forecast system. *Geoscience Model Development, 12*(3), 1087–1117. https://doi.org/10.5194/gmd-12-1087-2019

Joseph PV, Sijikumar S (2004) Intraseasonal variability of the low level jet stream of the Asian summer monsoon. Journal of Climate *17*(7), 1449–1458. https://doi.org/10.1175/1520-0442(2004)017<1449:IVOTLJ>2.0.CO;2.

Kang, I. S., Jin, E. K., & An, K. H. (2006). Secular increase of seasonal predictability for the 20th century. *Geophysical Research Letters, 33*, L02703.

Kang, I. S., Lee, J., & Park, C. K. (2004a). Potential predictability of summer mean precipitation in a dynamical seasonal prediction system with systematic error correction. *Journal of Climate, 17*(4), 834–844. https://doi.org/10.1175/1520-0442(2004)017%3c0834:PPOSMP%3e2.0.CO;2

Kang, I. S., Lee, J., & Park, C. K. (2004b). Potential predictability of summer mean precipitation in a dynamical seasonal prediction system with systematic error correction. *Journal of Climate, 17*, 834–844.

Kim, H. M., Webster, P. J., Curry, J. A., & Toma, V. E. (2012). Asian summer monsoon prediction in ECMWF System 4 and NCEP CFSv2 retrospective seasonal forecasts. *Climate Dynamics, 39*(12), 2975–2991. https://doi.org/10.1007/s00382-012-1470-5

Krishna Kumar K, Hoerling M, Rajagopalan B (2005) Advancing dynamical prediction of Indian monsoon rainfall. *Geophysics Research Letter 32*(8). https://doi.org/10.1029/2004GL021979.

Kumar, A., & Hoerling, M. P. (1995). Prospects and limitations of seasonal atmospheric GCM predictions. *Bulletin of the American Meteorological Society, 76*(3), 335–345. https://doi.org/10.1175/1520-0477(1995)076%3c0335:PALOSA%3e2.0.CO;2

Kumar, K. K., Rajgopalan, B., & Cane, M. K. (1999). On the weakening relationship between the Indian monsoon and ENSO. *Science, 284*(5423), 2156–2159. https://doi.org/10.1126/science.284.5423.2156

Lee, S. S., Lee, J. Y., Ha, K. J., Wang, B., & Schemm, J. K. E. (2011). Deficiencies and possibilities for long-lead coupled climate prediction of the Western North Pacific-East Asian summer monsoon. *Climate Dynamics, 36*, 1173–1188. https://doi.org/10.1007/s00382-010-0832-0

Pai, D. S., Sridhar, L., Rajeevan, M., Sreejith, O. P., Satbhai, N. S., Mukhopadhyay, B. (2014). Development of a new high spatial resolution (0.25° × 0.25°) long period (1901–2010) daily gridded rainfall data set over India and its comparison with existing data sets over the region. *Mausam 65*(1), 1–18.

Palmer, T. N., et al. (2004). Development of a European multimodel ensemble system for seasonal to interannual prediction (DEMETER). *Bulletin of the American Meteorological Society, 85*(6), 853–872. https://doi.org/10.1175/BAMS-85-6-853

Pandey, D. K., Rai, S., Shahi, N., & Mishra, N. (2015). Seasonal prediction of ISMR and relationship with EL-NIÑO and IOD in ECMWF system 4 coupled model. *Climate Change, 1*(4), 447–455.

Paparrizos, S., Smolenaars, W., Gbangou, T., Slobbe, E. V., & Ludwig, F. (2020). Verification of Weather and Seasonal Forecast Information Concerning the Peri-Urban Farmers' Needs in the Lower Ganges Delta in Bangladesh. *Atmos, 11*(10), 1041. https://doi.org/10.3390/atmos11101041

Pillai, P. A., Rao, S. A., Das, R. S., Dhakate, S. K., & A,. (2018a). Potential predictability and actual skill of Boreal Summer Tropical SST and Indian summer monsoon rainfall in CFSv2-T382: Role of initial SST and teleconnections. *Climate Dynamics, 51*(1), 493–510. https://doi.org/10.1007/s00382-017-3936-y

Pillai, P. A., Rao, S. A., George, G., Rao, D. N., Mahapatra, S., Rajeevan, M., Dhakate, S., & Salunke, S. (2017). How distinct are flavors of El-Niño in retrospective forecasts of climate forecast system version2 (CFSv2)? *Climate Dynamics, 48*(11), 3829–3854. https://doi.org/10.1007/s00382-016-3305-2

Pillai, P. A., Rao, S. A., Ramu, D. A., Pradhan, M., & George, G. (2018b). Seasonal prediction skill of Indian summer monsoon rainfall in NMME models and monsoon mission CFSv2. *International Journal of Climatology, 38*, e847–e861. https://doi.org/10.1002/joc.5413

Pokhrel, S., Rahaman, H., Parekh, A., Subodh, K. S., Dhakate, A., Chaudhari, H. S., & Gairola, R. M. (2012). Evaporation–precipitation variability over Indian Ocean and its assessment in NCEP Climate Forecast System (CFSv2). *Climate Dynamics, 39*, 2585–2608. https://doi.org/10.1007/s00382-012-1542-6

Pokhrel, S., Saha, S. K., Dhakate, A., Rahman, H., Chaudhari, H. S., Salunke, K., Hazra, A., Sujith, K., & Sikka, D. (2016). Seasonal prediction of Indian summer monsoon rainfall in NCEP CFSv2: Forecast and predictability error. *Climate Dynamics, 46*(7–8), 2305–2326.

Pradhan, P. K., Prasanna, V., Lee, D. Y., & Lee, M. I. (2015). El Niño and Indian summer monsoon rainfall relationship in retrospective seasonal prediction runs: Experiments with coupled global climate models and MMEs. *Meteorology and Atmospheric Physics, 128*, 97–115. https://doi.org/10.1007/s00703-015-0396-y

Rajeevan, M., & Pai, D. S. (2007). On the El Niño-Indian monsoon predictive relationships. *Geophysical Research Letters, 34*(4), L04704. https://doi.org/10.1029/2006GL028916

Rajeevan, M., Unnikrishnan, C. K., & Preethi, B. (2012). Evaluation of the ENSEMBLES multi-model seasonal forecasts of

Indian summer monsoon variability. *Climate Dynamics, 38*, 2257–2274. https://doi.org/10.1007/s00382-011-1061-x

Ramu, D. A., Sabeerali, C. T., Chattopadhyay, R., Rao, D. N., George, G., Dhakate, A. R., Salunke, K., Srivastava, A., & Rao, S. A. (2016). Indian summer monsoon rainfall simulation and prediction skill in the CFSv2 coupled model: Impact of atmospheric horizontal resolution. *Journal of Geophysics Research Atmosphere, 121*(5), 2205–2221. https://doi.org/10.1002/2015JD024629

Rao, S. A., Chaudhari, H. S., Pokhrel, S., & Goswami, B. N. (2010). Unusual Central Indian drought of summer monsoon 2008: Role of southern tropical Indian Ocean warming. *Journal of Climate, 23*(19), 5163–5174. https://doi.org/10.1175/2010JCLI3257.1

Rasmusson, E. M., & Carpenter, T. H. (1983). The relationship between eastern equatorial Pacific sea surface temperatures and rainfall over India and Sri Lanka. *Monthly Weather Review, 1*, 517–528. https://doi.org/10.1175/1520-0493(1983)111%3c0517:TRBEEP%3e2.0.CO;2

Rayner, N. A., Parker, D. E., Horton, E. B., Folland, C. K., Alexander, L. V., Rowell, D. P., Kent, E. C., & Kaplan, A. (2003). Global analyses of sea surface temperature, sea ice, and night marine air temperature since the late nineteenth century. *Journal of Geophysical Research, 108*(D14), 4407. https://doi.org/10.1029/2002JD002670

Rowell, D. P., Folland, C. K., Maskell, K., & Ward, M. N. (1995). Variability of summer rainfall over tropical North Africa (1906–92): Observations and modeling. *Quarterly Journal Royal Meteorological Society, 121*(523), 669–704. https://doi.org/10.1002/qj.49712152311

Saha, S., et al. (2006). The NCEP Climate Forecast System. *Journal of Climate, 19*(15), 3483–3517. https://doi.org/10.1175/JCLI3812.1

Saha, S. K., et al. (2013). Improved simulation of Indian summer monsoon in latest NCEP climate forecast system free run. *International Journal of Climatology, 34*(5), 1628–1641. https://doi.org/10.1002/joc.3791

Saha, S., et al. (2014). The NCEP Climate Forecast System Version 2. *Journal of Climate, 27*(6), 2185–2208. https://doi.org/10.1175/JCLI-D-12-00823.1

Saji, N. H., Goswami, B. N., Vinayachandran, P. N., & Yamagata, T. (1999). A dipole mode in the tropical Indian Ocean. *Nature, 401*, 360–363. https://doi.org/10.1038/43854

Singh, B., Cash, B., & Kinter, J. L., III. (2019). Indian summer monsoon variability forecasts in the North American multimodel ensemble. *Climate Dynamics, 53*(12), 7321–7334.

Singh, P., Vasudevan, V., Chowdary, J. S., & Gnanaseelan, C. (2014). Subseasonal variations of Indian summer monsoon with special emphasis on drought and excess rainfall years. *International Journal of Climate, 35*(4), 570–582. https://doi.org/10.1002/joc.4004

Wang, B., Lee, J. Y., Kang, I. S., et al. (2009). Advance and prospectus of seasonal prediction: Assessment of the APCC/CliPAS 14-model ensemble retrospective seasonal prediction (1980–2004). *Climate Dynamics, 33*, 93–117. https://doi.org/10.1007/s00382-008-0460-0

Wang, B., Lee, J. Y., Kang, I. S., Shukla, J., Kug, J. S., Kumar, A., Schemm, J., Luo, J. J., Yamagata, T., & Park, C. K. (2008). How accurately do coupled climate models predict the Asian-Australian monsoon interannual variability? *Climate Dynamics, 30*, 605–619.

Webster, P. J., & Yang, S. (1992). Monsoon and ENSO: Selectively Interactive Systems. *Quarterly Journal Royal Meteorological Society, 118*(507), 877–926. https://doi.org/10.1002/qj.49711850705

Wilks, D. S. (2006). Frequentist Statistical Inference. *Statistical methods in the atmospheric sciences* (3rd ed., Vol. 100, pp. 133–185). Elsevier Publishers.

Xie, P., & Arkin, P. A. (1997). Global Precipitation: A 17-year monthly analysis based on Gauge observations, Satellite estimates, and Numerical Model Outputs. *Bulletin of the American Meteorological Society, 78*(11), 2539–2558.

(Received May 27, 2022, revised October 1, 2022, accepted November 14, 2022, Published online December 5, 2022)